Supporting information

3D Morphology of Bimodal Porous Copper with Nano-Sized and Micron-Sized Pores to Enhance Transport Properties for Functional Applications

Lijie Zou [a, b], Mingyuan Ge [c], Jianming Bai [c], Chonghang Zhao [b], Hao Wang [a], Xianghui Xiao[c], Hui Zhong [d], Sanjit Ghose [c], Wah-Keat Lee[c], Qiang Shen [a]*, Fei Chen [a]*, Yu-chen Karen Chen-Wiegart [b, c]*

[a] State Key Lab of Advanced Technology for Materials Synthesis and Processing, Wuhan University of Technology, Wuhan 430070, China

[b] Department of Materials Science and Chemical Engineering, Stony Brook University, Stony Brook, New York 11794, United States

[c] National Synchrotron Light Source - II, Brookhaven National Laboratory, Upton, New York 11973, United States

[d] Department of Joint Photon Science Institute, Stony Brook University, Stony Brook, New York 11794, United States

*corresponding authors: Karen.Chen-Wiegart@stonybrook.edu; chenfei027@whut.edu.cn; sqqf@whut.edu.cn

Further information on refinement analysis results

The synchrotron X-ray powder diffraction (XPD) refinement results of six different precursor alloys are shown in Figure S 1. The refinement results provide the information of phase composition, crystal structure, lattice parameter, phase density, weight percent and volume percent of each phase, as shown in Table S 1. Because the atomic radius of Cu and Fe are quite similar, they cannot be distinguished accurately in XPD beamline. When doing refinement, the definite crystal structures of CuFeAl phase are used as models and locally adjusting the atomic site occupancy of Cu, Fe and Al in each phase to make the total relative ratio of Cu, Fe and Al similar to that in initial precursor alloys. Therefore, the atomic site occupancy is only a reference. Moreover, although there is an unidentified phase in $Al_{30}Fe_{45}Cu_{25}$ alloy, the intensity of this unknown phase very low, so that it did not have

much effect on the other three phases during the refinement. Table S 1 showed that for the phases with the same crystal structure in various alloys, the atomic site occupancy is different.

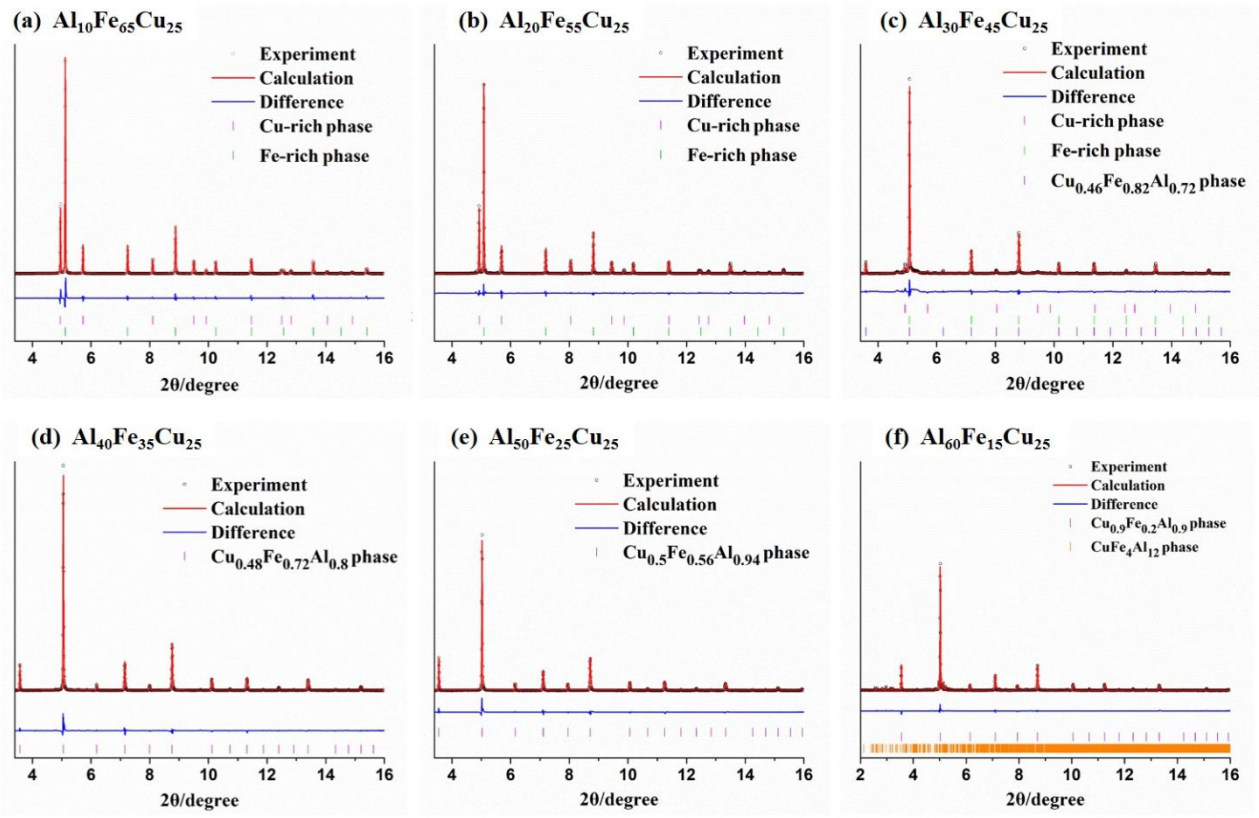

Figure S 1 The synchrotron X-ray powder diffraction (XPD) refinement results of six different precursor alloys: (a) $Al_{10}Fe_{65}Cu_{25}$, (b) $Al_{20}Fe_{55}Cu_{25}$, (c) $Al_{30}Fe_{45}Cu_{25}$, (d) $Al_{40}Fe_{35}Cu_{25}$, (e) $Al_{50}Fe_{25}Cu_{25}$, (f) $Al_{60}Fe_{15}Cu_{25}$.

Table S 1 - Phases quantification of six different precursor alloys obtained from synchrotron X-ray

Alloy	Phase	Crystal structure	Lattice parameter (Å)	Phase ratio (%)	Atomic site occupancy			R_{WP} (%)
					Cu	Fe	Al	
$Al_{10}Fe_{65}Cu_{25}$	Cu-rich	Fm-3m	a=b=c=3.64	30.85	0.60	0.30	0.10	14.7
	Fe-rich	Im-3m	a=b=c=2.88	69.15	0.07	0.89	0.20	
$Al_{20}Fe_{55}Cu_{25}$	Cu-rich	Fm-3m	a=b=c=3.67	32.88	0.50	0.30	0.20	13.4
	Fe-rich	Im-3m	a=b=c=2.90	67.12	0.13	0.67	0.20	
$Al_{30}Fe_{45}Cu_{25}$	Cu-rich	Fm-3m	a=b=c=3.67	4.92	0.58	0.16	0.26	19.9
	Fe-rich	Im-3m	a=b=c=2.91	50.69	0.15	0.75	0.10	
	$Cu_{0.46}Fe_{0.82}Al_{0.72}$	Pm-3m	a=b=c=2.91	44.38	0.45	0.70	0.85	
	unknown	/	/	/	/	/	/	
$Al_{40}Fe_{35}Cu_{25}$	$Cu_{0.48}Fe_{0.72}Al_{0.8}$	Pm-3m	a=b=c=2.92	100	0.48	0.72	0.80	16.3
$Al_{50}Fe_{25}Cu_{25}$	$Cu_{0.5}Fe_{0.56}Al_{0.94}$	Pm-3m	a=b=c=2.93	100	0.50	0.56	0.94	
$Al_{60}Fe_{15}Cu_{25}$	$Cu_{0.9}Fe_{0.2}Al_{0.9}$	Pm-3m	a=b=c=2.94	69.61	0.90	0.20	0.90	11.9
	$CuFe_4Al_{12}$	C2/m	a=15.55, b=7.99, c=12.51	30.39	6	24	72	

Composition of bimodal porous Cu after dealloying of Cu-Fe-Al alloys

The X-ray diffraction results of porous Cu after dealloying of six different Cu-Fe-Al precursor alloys are shown in Figure S 2. Only Cu phase diffraction peaks (with high intensity) and $Cu_{2+1}O$ phase diffraction peaks (with very low intensity) were detected in the XRD patterns of porous Cu. The results show that Fe and Al have been fully dissolved in the 5 wt% sulfuric acid (H_2SO_4) aqueous solution at 90 °C, and a small amount of Cu was oxidized during the dealloying process.

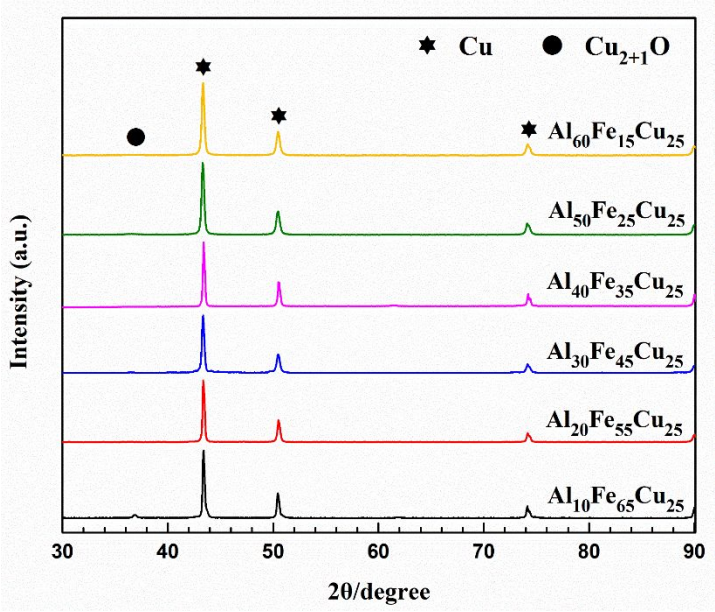

Figure S 2 The X-ray diffraction (XRD) results of porous Cu after dealloying of six different precursor alloys: $Al_{10}Fe_{65}Cu_{25}$, $Al_{20}Fe_{55}Cu_{25}$, $Al_{30}Fe_{45}Cu_{25}$, $Al_{40}Fe_{35}Cu_{25}$, $Al_{50}Fe_{25}Cu_{25}$, $Al_{60}Fe_{15}Cu_{25}$.

Average Size from the Pore Size Distribution by Gaussian Fitting

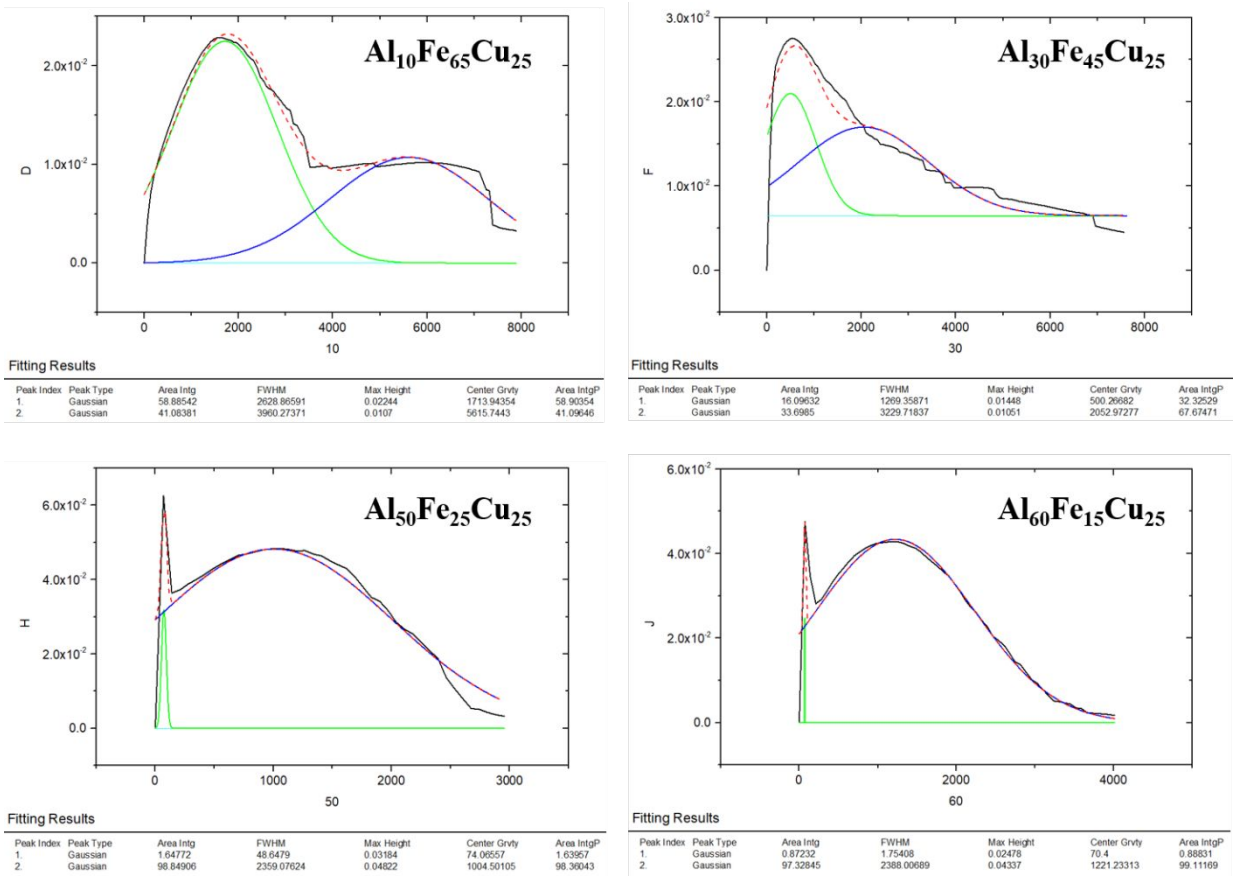

Figure S 3 – Gaussian fitting of pore size distribution

Table S 2 – Fitted results of average pore size and full width half maximum

Precursor Composition	Average Pore Size (Center Gravity) (nm)	Full Width Half Maximum (FWHM) (nm)
$Al_{10}Fe_{65}Cu_{25}$	1713 5616	2629 3960
$Al_{30}Fe_{45}Cu_{25}$	500 2053	1269 3230
$Al_{50}Fe_{25}Cu_{25}$	74 1005	49 2359
$Al_{60}Fe_{15}Cu_{25}$	70 1221	2 2388